

# We are IntechOpen, the world's leading publisher of Open Access books Built by scientists, for scientists

6,900

Open access books available

186,000

International authors and editors

200M

Downloads

Our authors are among the

154

Countries delivered to

TOP 1%

most cited scientists

12.2%

Contributors from top 500 universities



WEB OF SCIENCE™

Selection of our books indexed in the Book Citation Index  
in Web of Science™ Core Collection (BKCI)

Interested in publishing with us?  
Contact [book.department@intechopen.com](mailto:book.department@intechopen.com)

Numbers displayed above are based on latest data collected.  
For more information visit [www.intechopen.com](http://www.intechopen.com)



# Numerical Simulation for Vehicle Powertrain Development

Federico Millo, Luciano Rolando and Maurizio Andreatta  
*Politecnico di Torino,  
Italy*

## 1. Introduction

Increasing concerns about environmental issues, such as global warming and pollutant emissions, as well as the predicted scarcity of oil supplies have made energy efficiency and reduced pollutant emissions a primary selling point for automobiles. As a result, the design of vehicle powertrain becomes more challenging since it has to achieve these additional targets, without compromising other performance such as power, torque or fun to drive. In this context, thanks to the exponential growth of computational power, ground transportation industry has accepted the reality that fast, efficient, and cost effective engine and vehicle development necessitates the use of numerical simulation at every stage of the design process. Within the vehicle powertrain design and development process, three different levels of modelling can generally be found:

- *Detailed modelling*: it is performed during the research and early development stages. It is mainly focused on single powertrain components, such as for instance the internal combustion engine or the electric motor of a Hybrid Electric Vehicle (HEV), providing detailed information about their behaviour, while it cannot study the whole system.
- *Software in the Loop (SiL) modelling*: it is carried out later in the development cycle but often before production hardware is available. It has a global perspective and it can be used to evaluate vehicle performance. Moreover today SiL becomes popular in control system development, such as for instance in the development of HEVs energy management systems.
- *Hardware in the Loop (HiL) modelling*, which is conducted once production controllers are available.

Therefore, this chapter will provide a description of different methodologies which can support engineers in each phase of the vehicle powertrain design process. Starting from the description of different modelling approaches, the chapter will then go deeper into the analysis of numerical models for the main powertrain subsystems (such as for instance the internal combustion engine, the electric motors for HEVs, etc.).

Finally, two case studies of numerical simulation applied to powertrain development will be presented; the first focused on the evaluation of vehicle performance, paying particular attention to the engine behaviour under transient conditions, the second aiming instead to the assessment of the fuel economy potential of different Hybrid Electric Vehicle architectures.

## 2. Modelling methodology

Since one of the main objectives of vehicle models is to estimate the engine fuel consumption and pollutant emissions in different driving conditions, the next section will provide a brief description of the three most common modelling approaches suitable for this application.

A conventional powertrain, with a unique power source represented by an internal combustion engine will be considered for the sake of simplicity.

### 2.1 Kinematic approach

The kinematic approach is based on a backward methodology (see Fig. 1) where the input variables are the speed of the vehicle and the grade angle of the road (Genta, 1997). The engine speed can therefore be easily determined from simple kinematic relationships, starting from the wheel revolution speed and the total transmission ratio of the driveline, while the traction force that should be provided to the wheels to drive the vehicle according to the chosen speed profile can be calculated from the main vehicle characteristics (i.e. vehicle mass, aerodynamic drag and rolling resistance).

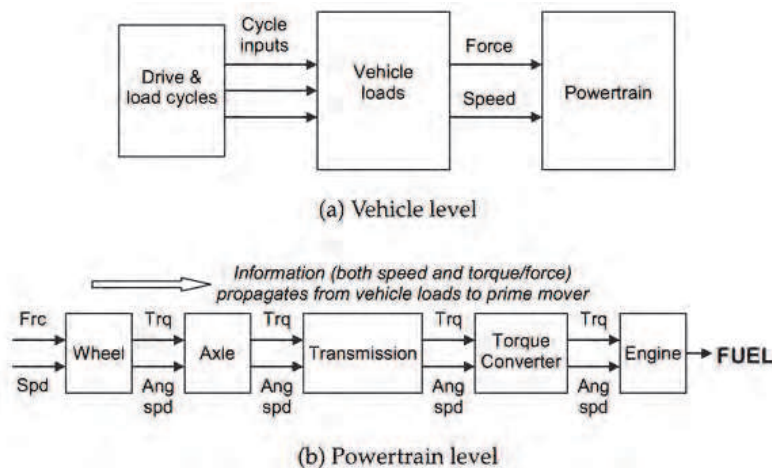


Fig. 1. Information flow in a kinematic or backward simulator (from Guzzella & Sciarretta, 2007).

Once both engine torque (or the Brake Mean Effective Pressure, BMEP) and speed have been determined, a 0D black box model of the engine (see following sections) can be used to find the instantaneous fuel consumption or emission rate, as shown in Fig.2. Finally, instantaneous fuel consumption and emission rate are integrated over the driving cycle to obtain cumulative data.

Obviously, this approach neglects all the dynamic phenomena considering transient conditions as a sequence of stationary states; therefore it is often used only for a first preliminary estimation of the fuel consumption or engine emissions of a motor vehicle, although the simulation results can differ significantly from the experimental data due to these simplifying assumptions. Moreover, the backward approach ensures that the driving profile will be exactly followed, but, on the other hand, there are no guarantees that a given vehicle will actually be able to meet the desired speed trace, since the power request is directly computed from the speed and it is not checked vs. actual powertrain capabilities (Guzzella & Sciarretta, 2007). Finally such an approach also neglects the thermal transient occurring after an engine cold start, which is, on the contrary, usually taken into account by most of the type approval driving cycles (such as NEDC, FTP, etc.).

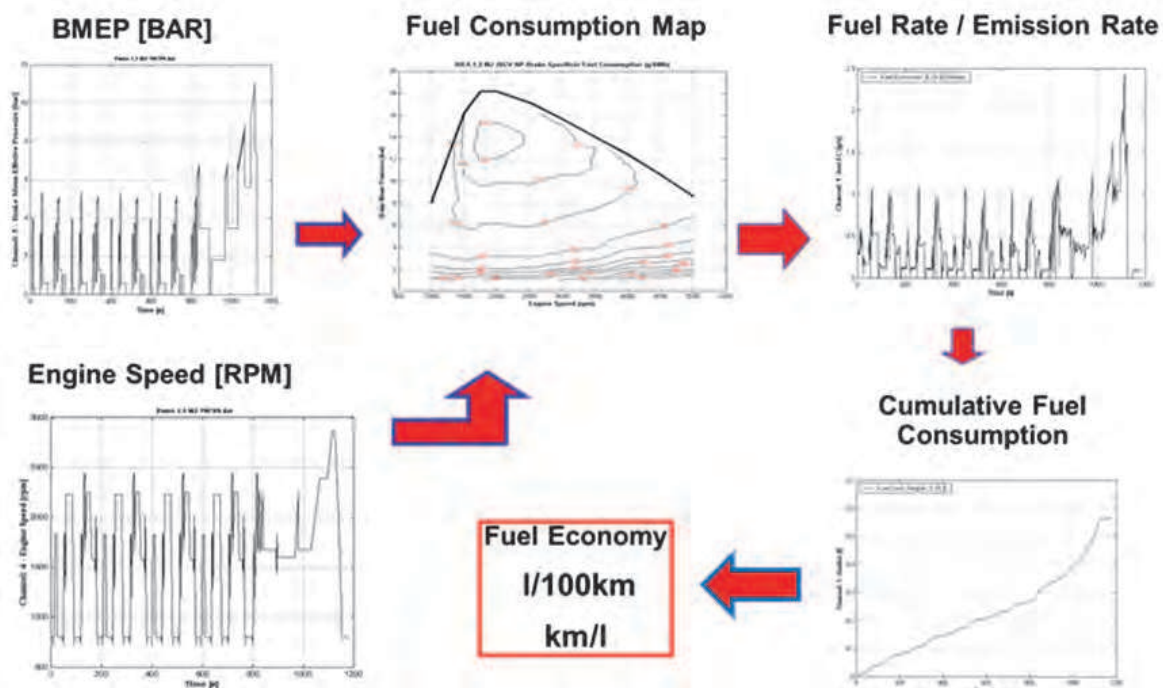


Fig. 2. Information flow in a backward model for motor vehicles fuel consumption calculation.

### 2.2 Quasi static approach

In the quasi static approach, a driver model (typically a PID) compares the target vehicle speed with the actual speed and generates a power demand profile in order to follow the target vehicle speed profile, by solving the longitudinal vehicle dynamics equation as shown in Fig.3 (Guzzella & Sciarretta, 2007; GAMMA TECHNOLOGY, 2009).

Once the torque and speed of the engine have been determined, fuel consumption or pollutant emissions can then be calculated by means of interpolation of engine maps, as for the kinematic methodology which was described in the previous section.

The simulation model can therefore be regarded as a “quasi-static” model, since, although system dynamics are taken into account, the behaviour of the main devices (ICE, EM, batteries) is described by means of steady state performance maps.

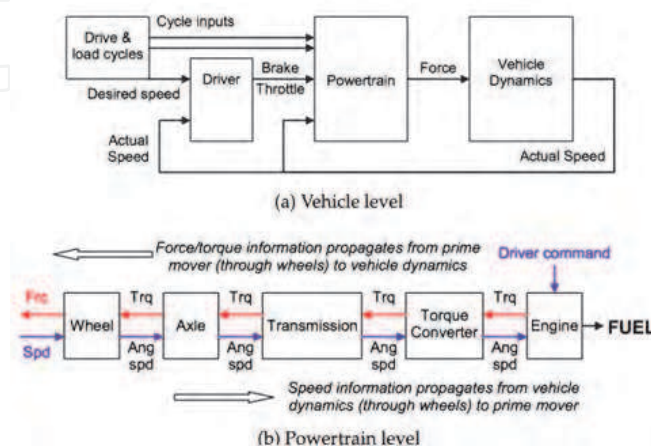


Fig. 3. Information flow in a quasi-static powertrain model (from Guzzella & Sciarretta, 2007).

Depending on the simulation targets, on the transient to be simulated and on the powertrain characteristics, a quasi-static approach can be suitable or not. For instance, for the evaluation of the fuel consumption of a vehicle equipped with a conventional powertrain on the NEDC, it can provide a reasonable accuracy, as shown in Fig. 4 (Vassallo et. al., 2007): as a matter of fact, since load and speed transients are relatively smooth for a conventional powertrain on the NEDC the simplifying assumptions of this method do not deteriorate significantly its prediction capabilities. Similar remarks could also be made as far as NO<sub>x</sub> emissions are concerned, also shown in Fig.4.

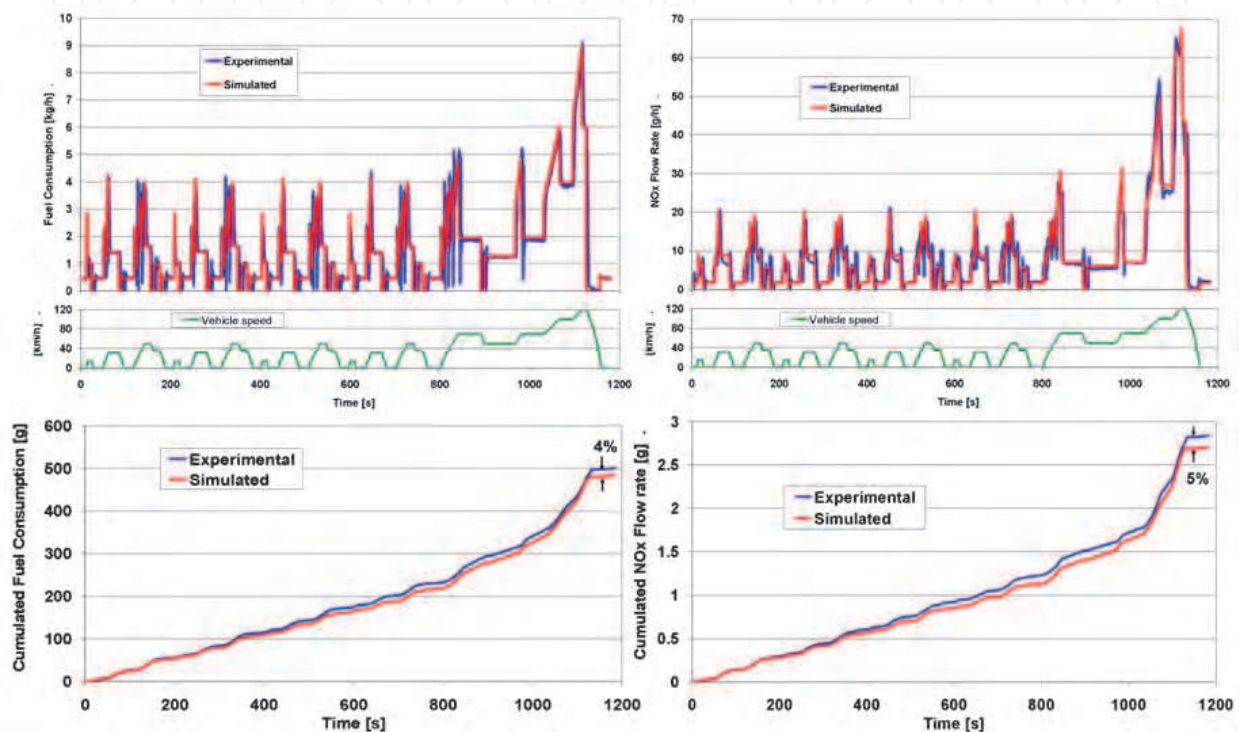


Fig. 4. Top: fuel consumption and NO<sub>x</sub> emission rate over warm NEDC cycle for a conventional powertrain. Bottom: cumulated fuel consumption and NO<sub>x</sub> emissions on the same driving cycle (from Vassallo et. al., 2007).

On the other hand, for the same driving cycle and for the same powertrain, the same approach does not provide satisfactory results when used to predict soot emissions, since for this kind of pollutant the acceleration transients and the related “turbo-lag” phenomena significantly contribute to the cycle cumulative emissions, thus requiring a more detailed engine simulation model, capable to properly capture also the engine transient behaviour. More details can be found in the case studies described in section 4.

### 2.3 Dynamic approach

Finally, in the fully dynamic approach, not only the longitudinal vehicle dynamics equation is solved to determine the engine speed and the torque demand, but also the internal combustion engine behaviour during transients is modelled by means of detailed OD or 1D fluid-dynamic models. For instance, for an internal combustion engine, the intake and exhaust systems can be represented as a network of ducts connected by junctions that represent either physical joints between the ducts, such as area changes or volumes, or subsystems such as the engine cylinder.

The solution of the equations governing the conservation of mass, momentum and energy of the flow for each element of the network can then be obtained using a finite difference technique.

In this way, even highly dynamic events, such as abrupt vehicle accelerations during tip-in manoeuvres can be properly and reliably simulated with a reasonable accuracy, as shown for instance in Pettiti et al., 2007.

### 3. Subsystems analysis

Regardless of the simulation approach chosen, the performance of a vehicle powertrain model strongly depends on the methodologies which are applied to describe each powertrain component. Therefore the next sections will provide a description of the most common modelling techniques for the following powertrain sub-systems:

- Tyre
- Transmission
- Internal Combustion Engine
- Electric Motor
- Energy Storage System

#### 3.1 Tyre

In most of the studies concerning vehicle powertrain, a detailed model of the vehicle dynamic is not required and its mathematical description can be limited to longitudinal motion neglecting the equations dealing with the lateral behaviour, (Andrzejewski & Awrejcewicz, 2005).

Obviously it is necessary to provide a model of the tyre which represents the link between the powertrain and the external environment, allowing the calculation of the forces at the interface between the wheel and the road surface. The simplest tyre model is a perfect rolling model in which the deformation of the tyre is neglected and the torque applied to the wheel shaft is transformed into a traction force considering a pure rolling motion between the tyre and the soil (Genta, 1997). According to this approach the dynamic response of the tyre can be approximated by a first order delay and the maximum force generated at the road interface can be assumed to be proportional to the vertical load on the wheel. The first order delay is useful to avoid numerical issues at very low vehicle speed, and to simulate (although in a quite approximate way) the tyre damping. The brakes are modelled as an additional torque that reduces the net torque acting on the tyre. Therefore the net torque acting on the wheel is:

$$T_{wh} = T_{shaft} - T_{brake} \quad (1)$$

Where  $T_{wh}$  is the wheel torque,  $T_{shaft}$  is the torque at the driveshaft, and  $T_{brake}$  is the braking torque. The effective traction force is then:

$$F_x = \frac{1}{1 + \tau_x s} \frac{T_{wh}}{R_e} \quad (2)$$

Where  $F_x$  is the longitudinal force at the ground,  $R_e$  the effective rolling radius,  $\tau_x$  a time constant that introduces a delay between the torque and the force and  $s$  is the Laplace variable. The wheel speed  $\omega$  is then:

$$\omega = \frac{V_{veh}}{R_e} \quad (3)$$

Being  $V_{veh}$  the longitudinal vehicle speed. The value of longitudinal force is determined by the vertical load acting on the wheel:

$$-F_z \mu_{x,max} \leq F_x \leq F_z \mu_{x,max} \quad (4)$$

Where  $F_z$  is the vertical force on the wheel, and  $\mu_{x,max}$  is the peak value of the road/tyre friction coefficient (usually around 0.8-0.9 for dry asphalt).

If the study purposes also require the dynamic response of the tyres a *semi non-linear* model developed by Pacejka (Genta, 1997; Andrzejewski & Awrejcewicz, 2005) can be taken into account.

Once the force generated at the road/wheel interface by each individual tyre is available, it is possible to introduce the vehicle equilibrium equation:

$$M_{eqv} \dot{V}_{veh} = \sum F_x - F_{roll} - F_{aero} - F_{grade} \quad (5)$$

where  $M_{eqv}$  is the vehicle equivalent mass,  $\dot{V}_{veh}$  is the vehicle longitudinal acceleration,  $F_x$  represents the traction and braking force generated by each tyre,  $F_{roll}$  is the rolling resistance,  $F_{aero}$  is the aerodynamic resistance,  $F_{grade}$  is the grade resistance. The terms in Eq. 5 can be determined as follows.

- **Rolling resistance:**

$$F_{roll} = c_{roll}(V_{veh}, p_{tyre}, \dots) M_{veh} g \cos \alpha \quad (6)$$

Where  $g$  is the gravity acceleration,  $\alpha$  is the road slope (so that  $M_{veh} g \cos \alpha$  is the vertical component of the vehicle weight) and  $c_{roll}$  is the rolling resistance coefficient which, in principle, is a function of vehicle speed, tyre pressure  $p_{tyre}$ , external temperature etc. (Genta, 1997). In most cases however,  $c_{roll}$  is assumed to be constant, or to be an affine function of the vehicle speed. In this case the approximation commonly used is:

$$c_{roll} = c_0 + c_1 V_{veh} + c_2 V_{veh}^2 + c_3 V_{veh}^3 \quad (7)$$

- **Aerodynamic resistance:**

$$F_{aero} = \frac{1}{2} \rho_{air} A_f C_d V_{veh}^2 \quad (8)$$

Where  $\rho_{air}$  is the air density,  $A_f$  the vehicle frontal area,  $C_d$  the aerodynamic drag coefficient.

- **Road slope:**

$$F_{grade} = M_{veh} g \sin \alpha \quad (9)$$

- **Inertia:**

$$F_{inertia} = M_{eqv} \cdot \dot{V}_{veh} \quad (10)$$

Where  $M_{eqv}$  is the vehicle equivalent mass that takes into account all the inertia of the driveline components and can be expressed as (if the transmission inertia can be neglected):

$$M_{eqv} = M_{veh} + J_{wheel} \frac{1}{R_e^2} + J_{eng} \frac{\tau_{gear}^2 \tau_{fd}^2}{R_e^2} \quad (11)$$

Where  $M_{veh}$  is the vehicle mass,  $J_{wheel}$  is the wheel inertia,  $J_{eng}$  is the engine inertia,  $\tau_{gear}$  is the transmission gear ratio and  $\tau_{fd}$  is the final drive gear ratio.

The aerodynamic and rolling resistances can be experimentally determined by means of a so called *coast-down test*, consisting in a free vehicle deceleration. Since in these conditions the deceleration is due only to the rolling and aerodynamic resistances, by measuring the instantaneous vehicle speed the total drag force acting on the vehicle can be determined. The resulting relationship is then usually fitted by a quadratic function of the vehicle speed (BOSCH, 2011):

$$F_{roll+aero} = C_0 + C_1 V_{veh} + C_2 V_{veh}^2 \quad (12)$$

Where  $C_0$ ,  $C_1$  and  $C_2$  are called "Coast-Down Coefficients".

### 3.2 Transmission

In a motor vehicle the term transmission or driveline refers to all the mechanical devices used to connect the engine to wheels. It may include clutches, torque converters, differential and, more generally, gears.

Since nowadays most of the European passenger cars are equipped with manual gearboxes, this section will focus on the description of these transmissions. They can be represented as gear couples the transmission ratio of which can change dynamically: gears are mechanical components, whose external interfaces are two mechanical connections representing input and output shafts; they can be modelled through their transmission ratios and through an efficiency function  $\eta$  (depending on gear ratio, revolution speed, and input torque) which takes into account all power losses due to friction. Since the speed ratio is fixed, being determined by kinematic constraints, the power losses imply the reduction of the torque at the output shaft:

$$\begin{cases} \omega_{out} = \frac{\omega_{in}}{\tau} \\ T_{out} = \eta \tau T_{in} \end{cases} \quad (13)$$

Where  $\omega$  is the revolution speed,  $T$  the torque,  $\tau$  the transmission ratio,  $\eta$  the gear efficiency and the subscripts *in* and *out* refer to the input and output shafts according to the power flow. The corresponding power loss is then calculated as:

$$P_{loss} = \omega_{in} T_{in} (1 - \eta) \quad (14)$$

The variable gear ratio signal deriving from the gear selection index (which is determined on the basis of the driving cycle schedule) is filtered with a 1<sup>st</sup> order transfer function that simulates the delay involved in the actual procedure of gear shifting, that usually takes a few tenths of second to be completed (Serrao, 2009).

In vehicles equipped with manual transmissions, during gear shift phases in which the vehicle and the engine speeds have to be kinematically decoupled a clutch is needed.

Dry or wet friction clutches have no torque amplification capability and produce substantial losses especially during the first acceleration phase when the vehicle starts at zero velocity.

If the engine speed  $\omega_e$  is assumed to be constant during this drive away phase, the clutch dissipates the following amount of mechanical energy:

$$E_{clutch} = \frac{1}{2} J_v \omega_{c,0}^2 \quad (15)$$

Where  $\omega_{c,0}$  is the wheel velocity at which the clutch input speed  $\omega_e$  and the clutch output speed  $\omega_{gb}$  coincide for the first time. The inertia  $J_v$  includes the vehicle inertia and all inertia due to the rotating parts located downstream of the clutch. The amount of energy dissipated does not depend on the clutch torque profile during the clutch-closing process.

Finally, it should be pointed out that during all phases in which the clutch is slipping, the torque  $T_{gb}(t)$  at the gearbox input is not limited by the engine, but is defined by the clutch characteristics and by its actuation system. The clutch torque  $T_1(t)$  depends on the speed difference and the actuation input  $u(t)$ :

$$T_1(t) = T_{1,max}(\Delta\omega(t)) \cdot u(t), \quad 0 < u(t) < 1 \quad (16)$$

The maximum clutch torque  $T_{1,max}$  can then be approximated by:

$$T_{1,max}(t) = \text{sign}(\Delta\omega(t)) [T_b - (T_b - T_a) e^{-|\Delta\omega(t)|/\Delta\omega_0}] \quad (17)$$

The parameters  $\Delta\omega_0$ ,  $T_a$  and  $T_b$  must be determined experimentally, and they generally depend on the clutch temperature and wear (Guzzella & Sciarretta, 2007).

### 3.3 Engine

Depending on the application and on the required level of detail different simulation approaches can be used for the internal combustion engine modelling, as depicted in Fig. 5.

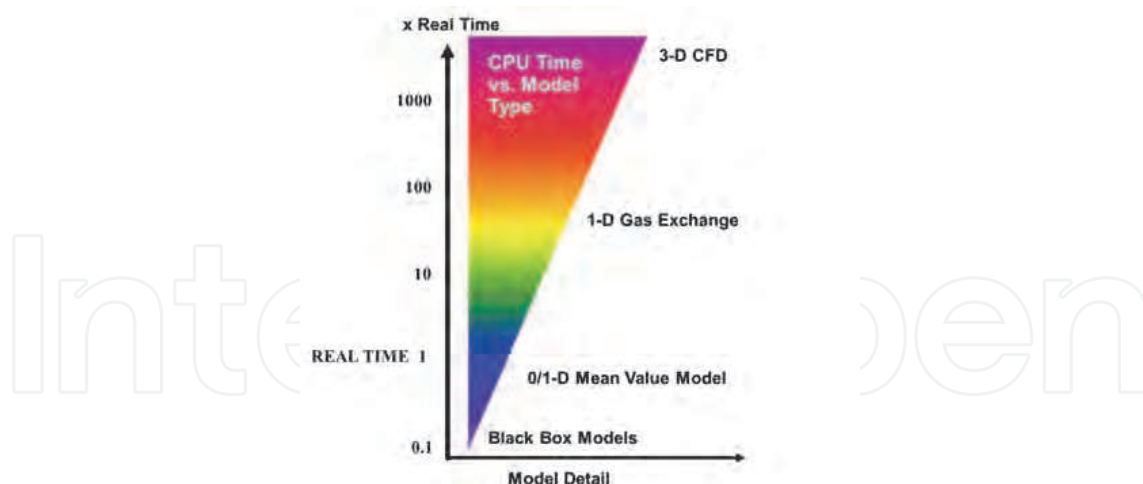


Fig. 5. Flowchart of the main engine modelling methodologies, showing model detail vs. computational time.

The most complete and detailed methodology is the 3D CFD: it is widely used for modelling flow dynamics in intake and exhaust systems of internal combustion engines, as well as for modelling in-cylinder phenomena such as gas flow through the intake and exhaust valves, direct fuel injection, mixture formation, combustion process etc. It can usually provide only component level details (such as for instance, pressure drops, flow distributions, fuel and air

mixing, etc.), but cannot usually provide a system level perspective, since, because the computational time increases with the system volume to be discretized, this approach is usually applied only to a specific engine component, such as for instance a single cylinder or a manifold, although some examples of application of 3D CFD modelling to a whole internal combustion engine, including intake and exhaust systems, have been reported in literature (Chiodi, 2010). In order to gain a system level perspective, 1D fluid-dynamic simulation tools are generally used (Keribar et al., 2000; Morel et al., 2006), in which the engine intake and exhaust systems are usually modelled as a network of ducts connected by junctions that may represent either physical joints between the ducts or subsystems such as the engine cylinder, and the solution of the equations governing the conservation of mass, momentum and energy of the flow for each element of the network is obtained using a finite difference technique. Typical applications of 1D fluid-dynamic models may include volumetric efficiency, torque and fuel consumption predictions under steady state operating conditions, as well as predictions of engine transient response to throttle tip-in and tip-out manoeuvres, turbocharging system response, etc.

Beyond these traditional uses, 1D simulations are today expanding in the area of control system modelling towards Software in the Loop (SiL), which is nowadays a popular activity in control system development prior to prototype hardware availability. At this level, 0D black-box models which follow a quasi-static approach based on experimental steady-state maps are currently the preferred options, due to their superior real-time capabilities. This approach is generally suitable for fuel consumption and emission calculations on type approval driving cycles, where transients are quite smooth and can be simulated by means of a sequence of stationary states.

However, 0D black box models, which neglect most (if not all) of the engine dynamic phenomena, are definitely unsuitable for the simulation of fast transients, such as for instance for the predictions of engine response to throttle tip-in and tip-out manoeuvres, or of turbocharging system response, for which 1D fluid-dynamic models would certainly be more appropriate, but are usually inapplicable because of their high computational time requirements.

For this reason the development of the so called “mean value” model seems to be the most valuable solution to combine the low computational requirements of black-box models with the accuracy of 1D models: the purpose of these models is the reduction of the complexity of a detailed 1D approach, while maintaining, at the same time, a physical description of the main phenomena in order to achieve the best compromise between detail level and computational requirements. Basically mean value models simplify both intake and exhaust systems in single equivalent volume where, as in a filling emptying model, the equation of conservation of energy and mass are applied. The separation of the thermodynamic properties between adjacent volumes is then possible thanks to restricting elements which imposes to the adjacent volumes a mass flow rate, which is calculated according to its characteristics and to the boundary conditions. Therefore the overall system behaviour, including turbocharger, is still represented although there is no detail about pressure wave dynamics (see also Fig. 6). Thanks to these features, the computational time is significantly reduced, with only limited impoverishment of the model detail, thus achieving an intermediate level between system black-box models and detailed engine models, as shown in Fig. 7.

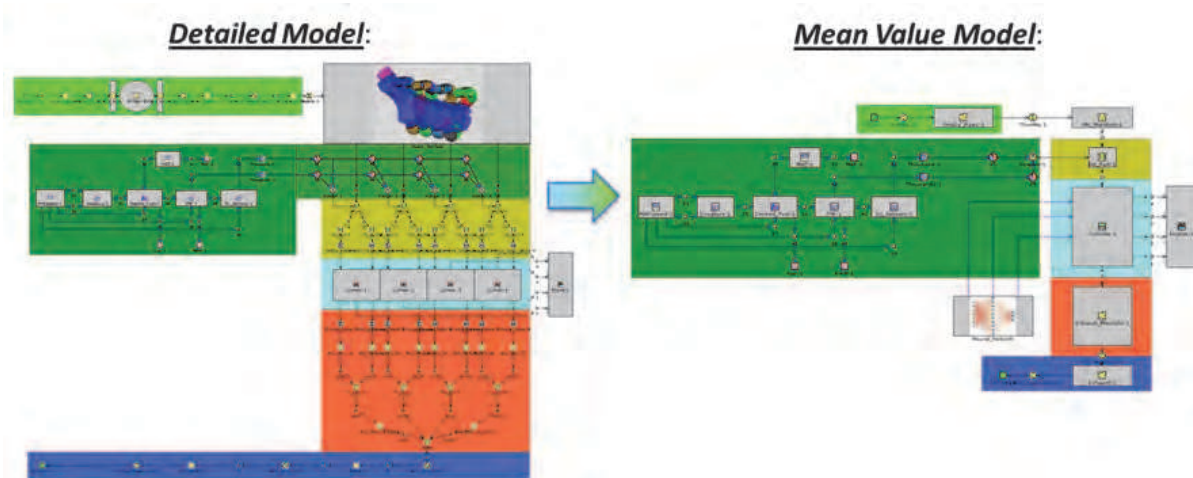


Fig. 6. Comparison between the structure of a detailed 1-D engine model (on the left) and a mean value model (on the right) – Example from Gamma Technology, 2009.

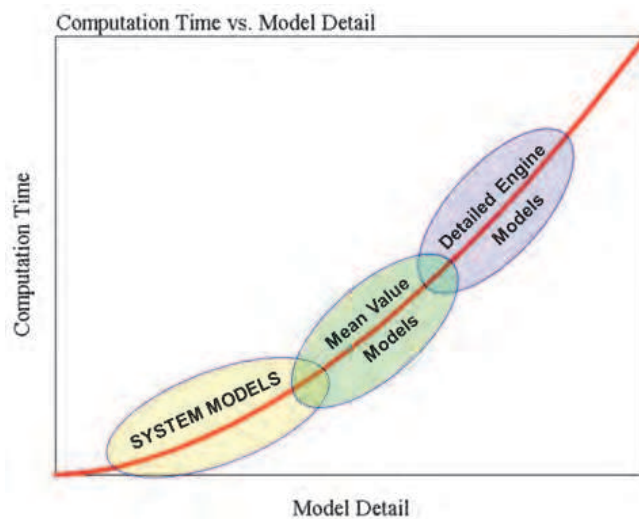


Fig. 7. Computational requirement vs. model detail for different engine modelling methodologies.

### 3.4 Electric motor

Nowadays the increasing share of HEVs and EVs in the automotive market makes electric machines (and in particular Electric Motors, EM) key components in vehicle powertrain development (Szumanowski, 2000).

Although the wide diffusion of electric machines in several areas of application has led to the development of different technologies (such as for instance AC and DC machines, synchronous vs. asynchronous motors, etc.) for powertrain development purposes electric machines can usually be modelled through a system-level approach similar to the 0D methodology previously described for the internal combustion engines, by means of torque and efficiency maps in which desired values of electrical power or torque are used as control inputs (see Fig. 8). Rotor inertia is the only dynamic element modelled, as the electrical dynamics are generally much faster. Thus, in most of the cases this quasi static modelling approach shows very good agreement with experimental data, and, as consequence, it is the

most widely used technique in HEVs powertrain modelling. The relation between the input and output power can be simply obtained as shown here below:

$$P_{electric} = \frac{P_{mech}}{\eta(\omega, T)} = \frac{\omega \cdot T}{\eta(\omega, T)} \quad (18)$$

Where  $P_{electric}$  is the EM electrical power,  $P_{mech}$  the EM mechanical power,  $T$  the EM torque,  $\omega$  the EM speed and  $\eta(\omega, T)$  the EM efficiency depending on torque and speed, as shown in Fig. 8.

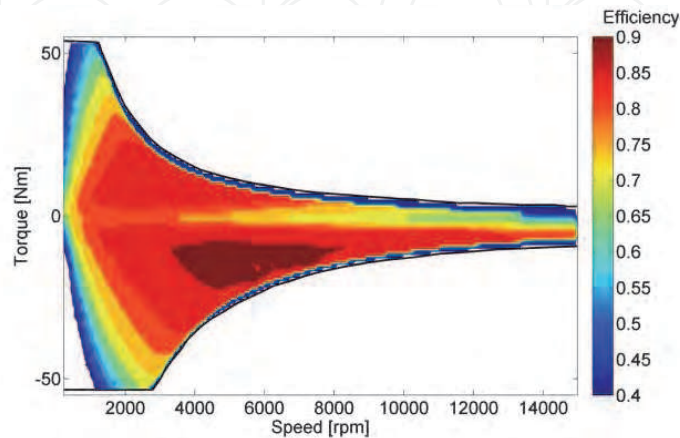


Fig. 8. Example of synchronous electric motor efficiency map.

### 3.5 Energy storage system: electrical battery

As for the electric machines, the relevance of electrical batteries in automotive applications has been rapidly increasing in the last years along with the rising interest for EVs and HEVs. Battery modelling is a complex task since all the main parameters that influence the battery properties (State Of Charge, voltage, current, temperature) are dynamically correlated to each other in a highly non-linear fashion.

Different modelling approaches can be adopted, depending on the detail level which is required and on the affordable computational requirement, but, regardless of the battery type (e.g. Ni-Mh, Li-Ion, etc.), the battery model purpose is generally to compute the battery State Of Charge or SOC, which is defined as the ratio between the actual charge stored in the battery and the maximum charge level, as shown in Eq. 19:

$$SOC(t) = \frac{Q(t)}{Q_{max}} = \frac{\int_0^t i(t) dt}{Q_{max}} \quad (19)$$

Where  $i(t)$  is the electric current flowing into or from the battery,  $Q(t)$  is the instantaneous charge stored in the battery and  $Q_{max}$  is the battery maximum charge.

The simplest battery model can then be obtained by means of the equivalent circuit shown in Fig. 9, consisting in an ideal voltage generator ( $U_{oc}$ ) in series with a resistor ( $R_i$ ). The Kirchhoff's law then yields the following equation:

$$U_2 = U_{oc} - R_i I_2 \quad (20)$$

The open circuit voltage  $U_{oc}$  depends on the State Of Charge SOC, and it can be computed either through performance maps experimentally measured, either through their linear approximation:

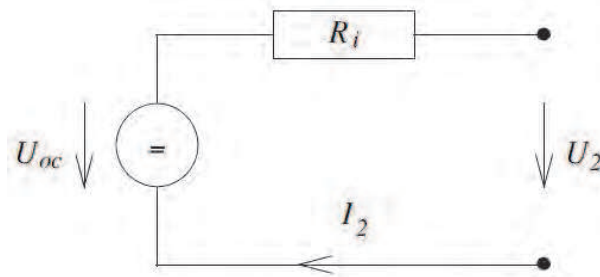


Fig. 9. Battery static model

$$U_{OC} = k_1 SOC(t) + k_2 \quad (21)$$

Where constants  $k_1$  and  $k_2$  depend on battery characteristics (i.e. number and connections of the cells, electrodes materials, etc.) but are generally independent from operating parameters, and are therefore constant with time.

The battery resistance  $R_i$  can then be split into the sum of three different contributions (Szumanowski, 2000):

- an ohmic resistance  $R_0$  representing all the ohmic resistances in the electrolyte, in the electrodes and in the battery interconnections;
- a charge transfer resistance  $R_{ct}$ , which is associated to the chemical reactions at the electrodes;
- a diffusion resistance  $R_d$  which models the diffusion of reactants and products in the layer between the electrode and the electrolyte.

These resistances values depend on the battery temperature, on the SOC and on the electric current in a highly non-linear fashion. Due to the difficulties in modelling the effects of these parameters, experimental data from constant current battery discharging test are often used to define a black box model of the battery resistance  $R_i$ .

The simple battery model above described is often referred to as a *static model*, since it does not take into account the dynamic behaviour of the battery during transient operating conditions. Whenever more complex models are needed for HEVs and EVs modelling, detailed reviews can be found in literature, such as for instance in González-Longatt, 2006.

#### 4. Case studies

The last section of this chapter will show two overviews on numerical studies concerning vehicle powertrain development. The former describes the build of a mean value engine model in order to investigate the dynamic performance of vehicles equipped with turbocharged diesel engines especially from the acceleration transient point of view. The latter shows an evaluation of different hybrid powertrains for an European mid-size passenger car, in order to obtain a preliminary assessment of their potentialities in terms of fuel consumption and pollutant emissions reductions.

##### 4.1 Mean value model for the analysis of turbolag phenomena in automotive diesel engines (Pettiti et al., 2007)

A positive perception of the vehicle performance by the driver is currently a key factor for customer acceptance of any new car model. So, particular attention must be paid to optimize the engine and vehicle behaviour during sudden acceleration transients, such as during the

tip-in manoeuvres which are usually employed to evaluate vehicle performance. However turbocharged engines, which are becoming more and more popular to satisfy the demand of high specific power outputs, suffer from the well-known "turbo-lag" phenomenon, showing a delayed response to an abrupt torque demand, due to the time which is required to speed-up the turbocharger so to obtain an adequate boost level.

This drawback is even more pronounced in diesel engines, because due to the insufficient boost level during acceleration transients, the amount of injected fuel has to be markedly reduced to avoid excessive smoke levels, thus resulting in poor engine performance. Therefore a simulation tool allowing a quick but reliable estimation of the impact of different design and calibration choices on vehicle performance during tip-in could be extremely helpful (Gambarotta, 2001; Canova & Gambarotta, 2002), because the simplest quasi static engine models are completely unsuitable, since they do not consider any transient phenomenon, as described in the previous sections. As a matter of fact, if these models were used to simulate tip-in manoeuvres, they would lead to an unacceptable overestimation of vehicle performance for any turbocharged engine. The aim of this work is therefore the design and development of a quite simple and flexible model for turbocharged diesel engines, able to simulate a tip-in manoeuvre with satisfactory accuracy. The model can be classified as a mean value model because it does not take into account the variation of the thermodynamic properties of the working gases within the engine cycle, like a detailed 1D model does, but it deals only with cycle-averaged thermodynamic quantities.

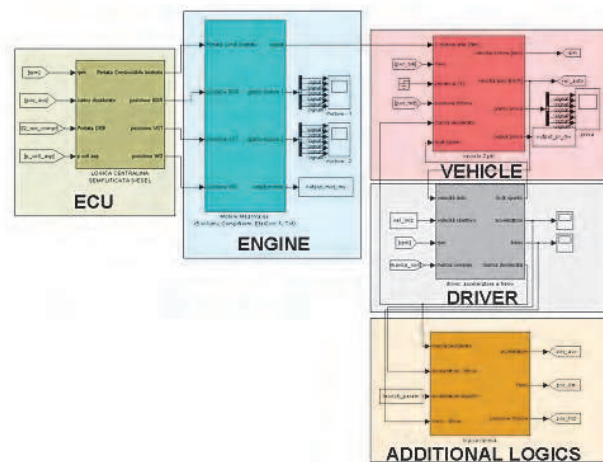


Fig. 10. Simulink vehicle mean value model: global layout

The global model layout is shown in Fig. 10: as one can see, it is made up of the following five main subsystems:

- ECU block
- Engine block
- Vehicle block
- Driver block
- Additional logics block

The ECU block receives as inputs the signals of the air mass flow meter, of the accelerator pedal position and of the current engine speed and it provides as outputs for the engine block the injected fuel mass, the VGT (Variable Geometry Turbine) and the EGR (Exhaust Gas Recirculation) actuators position. The engine model, which is the core block of the

system, takes into account main engine devices such as intake and exhaust systems, turbocharger and engine cylinder which are modelled through single control volumes.

As in filling and emptying models the equations of conservation of energy and mass are used to determine the thermodynamic state of each control volume, which is treated like an open thermodynamic system. Five control volumes were used in the model for the intake and exhaust systems, for the volume between compressor and intercooler and for intake and exhaust manifolds. The separation of the thermodynamic properties between adjacent volumes is possible thanks to restricting elements such as for instance valves, turbochargers, etc... The flow restricting element imposes to the adjacent volumes a mass flow rate, that is calculated according to its characteristics and to the boundary conditions.

The turbocharger was modelled through the efficiency and mass flow rate maps which are usually provided by the manufacturer. However, at the beginning of a tip-in manoeuvre, the initial turbocharger speed may easily fall to very low values, far from the range included in the original map of the compressor, requiring additional extrapolation routines. Finally, a simplified method was developed to quickly evaluate the turbocharger inertia, which is quite rarely supplied by the manufacturer together with the mass flow and efficiency maps.

The main output of the engine block is the delivered torque whose current value is passed to the vehicle block where the dynamic equilibrium equations for the driveline and the engine are solved in order to determine vehicle performance (i.e. longitudinal acceleration) and engine speed. This block also needs as inputs the brake and clutch positions, determined by the driver which is basically modelled through a PID controller.

The vehicle was simply modelled with two degree of freedom (one for the driveline and the other for the engine), i.e. a simple rigid driveline model was used. Despite its simplicity, this model showed to be suitable enough to simulate tip-in manoeuvres, mainly because in such conditions the turbocharged engine gradually delivers its torque, so that oscillating phenomena of the driveline are remarkably reduced if compared to naturally aspirated engines. Nevertheless at least a tyre model including slip would be necessary to improve simulation accuracy during “fast” tip-in manoeuvres, such as for instance second gear manoeuvres.

To assess the reliability and the accuracy of the model, an extensive comparison with experimental data was carried out. The test vehicle was an European compact car equipped with a 1.3 litre displacement VGT turbocharged diesel engine. Because a previous analysis carried out in Coltro, 2005 showed that the parameter which can be more closely related to the driver perception of vehicle performance is the vehicle acceleration pattern as a function of time, the comparisons were mainly focused on the abovementioned quantity. Moreover, this parameter can be particularly useful to highlight how the use of steady state models for evaluating the performance of turbocharged engines during tip-in transients may be inaccurate especially at the beginning of the manoeuvre. As one can see in Fig. 11 for a tip-in manoeuvre from 40 km/h in IV gear, the acceleration predicted with a steady model can be even double than the experimental value. On the contrary, the simulation carried out with the mean value model appears to be accurate, although a not negligible overestimation of the vehicle acceleration can still be noticed.

This can be ascribed to a corresponding overestimation of the boost pressure, as shown in Fig. 12. The possible reasons could be the absence of a fully detailed ECU control logic reproduction, as well as of a detailed model of the VGT actuator. Nevertheless, although an appreciable overestimation of the calculated vehicle acceleration can be observed also in this case, the accuracy of the prediction could be still considered as satisfactory.

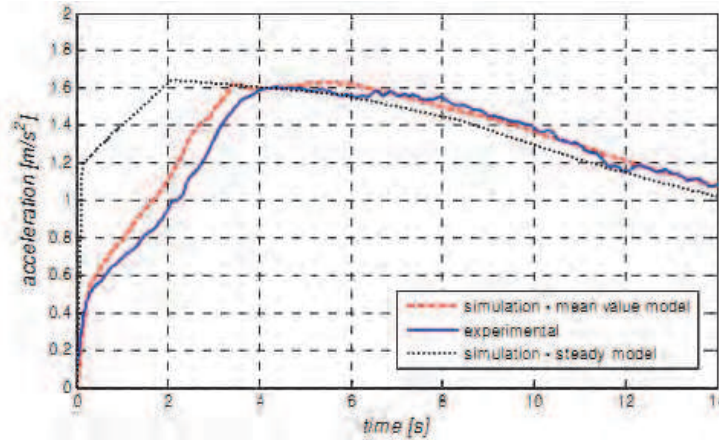


Fig. 11. Acceleration vs. time. Manoeuvre: tip-in from 40 km/h, IV gear.

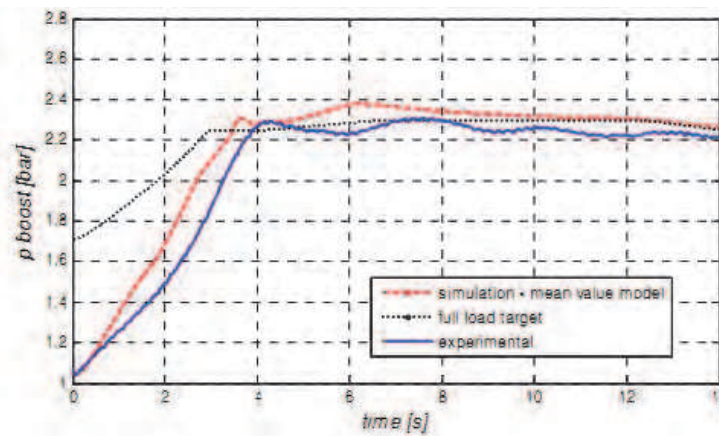


Fig. 12. Boost pressure vs. time. Manoeuvre: tip-in from 40 km/h, IV gear.

After assessing the model reliability and accuracy, the simulation tool could be used to evaluate the impact on vehicle performance of different design choices (such as, for instance, different gear ratios values) or calibration strategies (such as, for instance, the use of different “smoke maps” for fuel limitation during transients). As an example, the comparison of the acceleration patterns that could be obtained by means of three different smoke maps which limits the maximum injected mass is shown in Fig. 13.

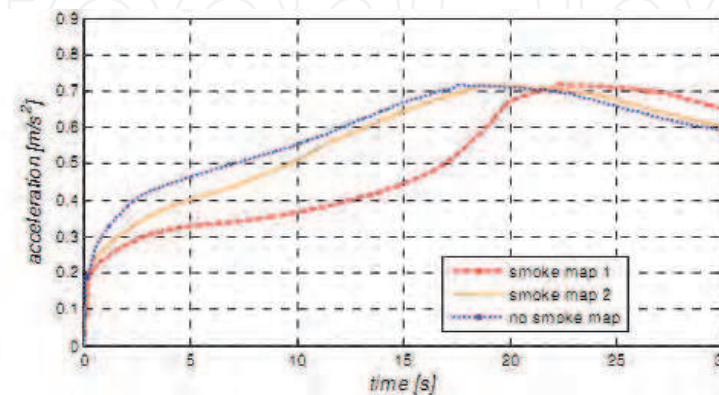


Fig. 13. (Effect of different smoke maps) Acceleration vs. time. Manoeuvre: tip-in from 60 km/h, VI gear.

In conclusion, the proposed model allows an easy and quick investigation on the impact on vehicle performance of several design parameters, such as, for instance, the inertia of the turbocharger or the gear ratios of the driveline. Moreover, the model is also suitable to evaluate the impact of different control strategies, concerning the smoke-related fuel injection limitation, the boost control through the VGT position and the EGR control.

#### 4.2 Development of a control strategy for complex light-duty diesel-hybrid powertrains (Millo et al., 2010)

The new CO<sub>2</sub> emission targets set by the EC (130 g/km over NEDC to be reached within 2012, and 95 g/km as a long term goal for 2020) are extremely demanding, especially for the long term target.

For an “average” European passenger car (compact size, about 1300 kg mass) the energy requested over NEDC can be estimated approximately equal to 0.4 MJ/km, that means that engine average efficiencies values around 32-33% will be required to reach the 95 g/km target (assuming a “pure powertrain” approach to the CO<sub>2</sub> target achievement, that is, without considering possible benefits coming from reduction in rolling resistance due to “green” tyres, aerodynamics improvements, vehicle body lightening, etc.).

However, even if remarkable improvements have been achieved in the last decade, it should be noted that over most of the NEDC the ICE is operated at low load, and thus with poor efficiency, thus making the 95 g/km CO<sub>2</sub> target far beyond current system capabilities. Consequently, it seems that a breakthrough from current technologies will be mandatory and coupling the high efficiency levels of diesel engines with the fuel saving potentials offered by hybridization could undoubtedly represent a valuable option. Nevertheless, despite these impressive potentialities, although diesel propulsion systems could undoubtedly add further benefits to Hybrid Electric Vehicles the high values of efficiencies that can be already attained by conventional diesel vehicles may make more difficult the development of hybridization strategies enabling further improvements in a cost effective way (Cooper et al., 2009).

Furthermore, some hybridization strategies aiming only to reach low fuel consumption targets may lead to unbearable penalties in terms of emissions, especially for NO<sub>x</sub>, and the add-up of the costs of hybrid and aftertreatment technologies which could be needed to meet future emissions regulations could seriously limit Diesel HEVs growth.

A careful analysis is therefore required in order to properly evaluate the potentialities of different hybrid architectures, taking into account also possible peculiar issues that may hinder their widespread application. Different degrees of hybridizations, from micro to mild hybrids, and different energy management systems were therefore evaluated in this work through numerical simulation, in order to obtain a preliminary assessment of the potentialities of different hybrid systems for the European passenger car market.

Four different hybrid architectures were considered (see Fig. 14):

- **Architecture A.** It corresponds to a typical medium size European passenger car, equipped with a Common Rail DI diesel engine (1.6 litre displacement) and a Manual Transmission (MT) gearbox.
- **Architecture B.** It is a Micro Hybrid with a Belt Alternator Starter (BAS). A small (2kW) Motor Generator Unit (MGU) is coupled to the internal combustion engine by means of a belt thus allowing the replacement of all the functionalities of both the starter and the alternator of the conventional vehicle.

- **Architecture C.** It features a Flywheel Alternator Starter (FAS): the Motor Generator Unit is installed between the engine and the gearbox and the electric power installed is one order of magnitude greater (18 kW) than the BAS. Two different variants were analysed: while the first one (which will be referred to as C1) features one clutch only located between the FAS and the gearbox, the second one (which will be referred to as C2) features a further clutch between the ICE and the FAS.
- **Architecture D.** It features the same Motor Generator Unit as architecture C, but coupled with a fixed transmission ratio to the output shaft of the gearbox. In this case the electric machine must be designed with quite different features, because it cannot benefit of the torque multiplication factor provided by the transmission, but will anyway be connected to the driveline by means of a dedicated gear with a transmission ratio equal to 5. Therefore the MGU power was reduced to 15 kW, while its maximum speed was increased up to 18000 rpm.
- **Architecture E.** It features the same 18 kW electric machine as architecture C, but connected to one of the primary shafts of a Dual Clutch Transmission (DCT). This provides an additional degree of freedom because the energy management system can choose the MGU gear ratio when the ICE torque flows through the other shaft in order to achieve further fuel consumption savings.

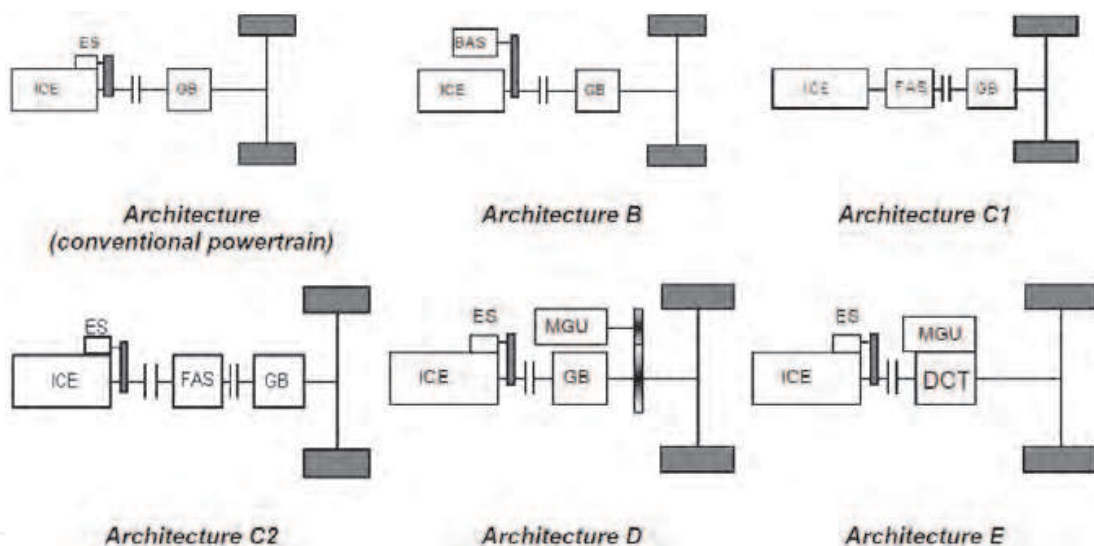


Fig. 14. Hybrid Electric Vehicles architectures (B, C, D and E) and reference conventional powertrain A

For all hybrid architectures, except the Micro Hybrid B, a Li-Ion battery constituted by 64 cells with 25 Wh energy capacity, and 730 W peak power each, for a total energy capacity of 1600 Wh was considered. A mean charge-discharge efficiency of 0.9 was considered.

HEVs simulations have been carried out with a vehicle model developed in the GT-Drive environment (GAMMA TECHNOLOGY, 2009; Morel et al., 2000), exploiting the quasi-static approach described in the previous sections. Fuel Consumption and engine out NOx emission were evaluated over the NEDC driving cycle on the basis of performance maps (see Fig. 15) neglecting warm-up phenomena due to lack of experimental data concerning the different engine calibration strategies adopted during a cold start. Moreover, since NOx emissions alone were evaluated (because they usually represent the major constraint for diesel hybridization strategies) and no NOx aftertreatment device was considered, engine-out emissions only were evaluated, and no aftertreatment model was used.

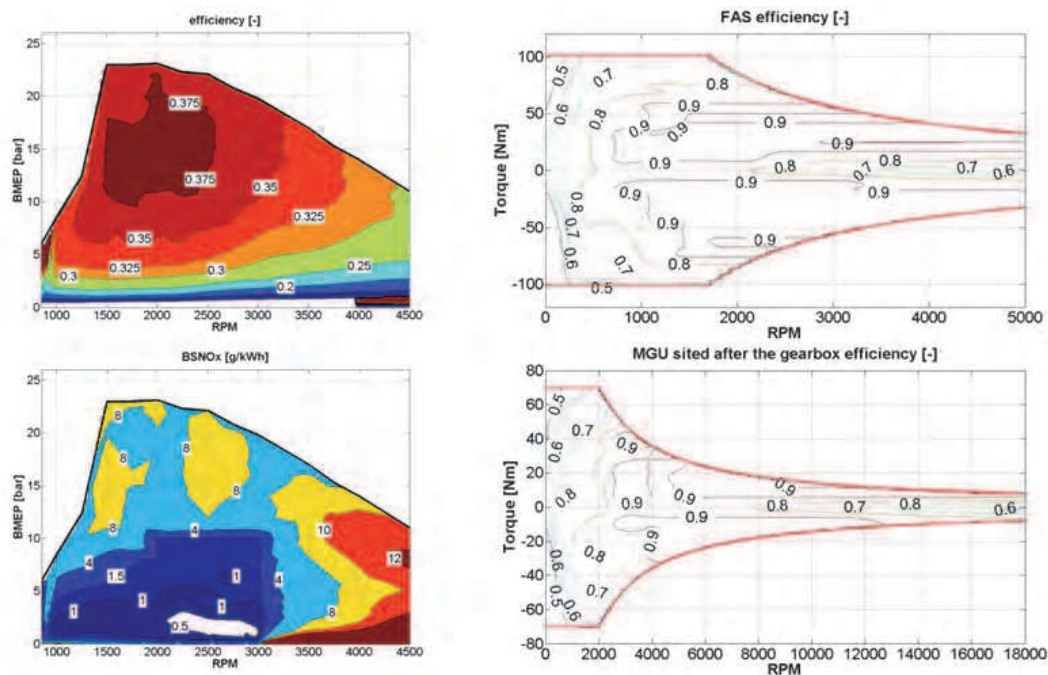


Fig. 15. Performance Maps – Left: Engine Efficiency and BSNOx maps. Right: MGUs efficiency maps.

Different power sources management strategies may be enabled depending on the hybrid architecture, as shown in Table 1. The base function enabled by the architecture B is the Stop&Start strategy. With the increase of electrical power available (architectures C, D and E), more options become available, from electrical power assistance during acceleration transients to improve vehicle performance (e-Boost), to regenerative braking. A larger battery allows also the “mild hybrid power management” strategy: whenever the State of Charge (SOC) of the battery is above a certain level, the pure electric mode is maintained until a proper power and/or vehicle speed threshold is exceeded, thus eliminating the ICE operations in the low load region which is characterized by poor efficiency figures.

Moreover, a further strategy specifically targeted to achieve a reduction of NOx emissions for the diesel powertrain can also be implemented, by using the MGU to assist the ICE even during the moderate vehicle acceleration prescribed by the NEDC driving cycle, in order to cut off the power peaks that are responsible of high NOx emissions rates. This strategy was specifically developed to solve a typical issue of diesel hybrids, that is the increase in NOx emissions produced by hybridization strategies aiming only to reach low fuel consumption targets by means of load point shift techniques.

	B	C	D	E
Start&Stop	√	√	√	√
e-Boost		√	√	√
Regenerative Braking		√	√	√
NOx cut		√	√	√
Mild Hybrid Power management		√	√	√

Table 1. Hybrid functionalities enabled depending on the hybrid architecture.

It should be pointed out that all the above mentioned strategies share a common target of a neutral battery energy balance at the end of the driving cycle, with a SOC variation compared to the initial value smaller than 1% of chemical energy consumed during the driving cycle.

The potential of the different hybrid architectures in terms of fuel consumption reduction over the NEDC has been firstly evaluated by applying to all architectures, except architecture B, a mild hybrid power management strategy with the purpose of achieving the lowest fuel consumption that will be referred to as “conventional”, since it encompasses start&stop, regenerative braking and load point shift with a target of lowest fuel consumption, but without any specific attention for NOx emissions, which undoubtedly represent the Achille’s heel of these solutions.

Afterwards, further investigations were carried out considering a “NOx cut” strategy. Fig. 16 and Fig. 17 show the main results obtained with the two different strategies.

The micro-hybrid architecture B, that only allows a simple Stop&Start, is capable to provide a 6% fuel consumption saving and a roughly equal NOx emissions reduction, thanks to the elimination of the idle phases.

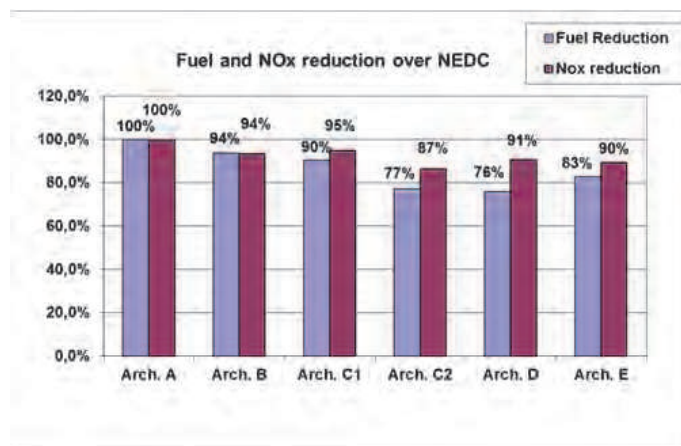


Fig. 16. Fuel consumption and NOx emissions reduction over NEDC for different diesel hybrid architectures with a “conventional” energy management strategy.

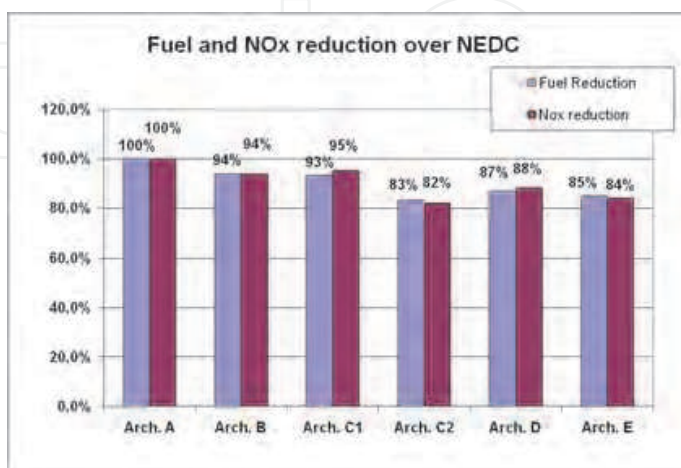


Fig. 17. Fuel consumption and NOx emissions reduction over NEDC for different diesel hybrid architectures with a “NOx cut” strategy.

On the other hand, the mild-hybrid architectures C, D and E, thanks to the higher electric power installed, increase significantly the fuel saving capabilities, reducing the fuel consumption up to 23-24% for architectures C2 and D, while allowing also an appreciable 10% average reduction of NO<sub>x</sub> emissions. The remarkable improvements in powertrain efficiency that can be achieved with architectures C2 and D are mainly due, in addition to the start&stop and regenerative braking savings, to the application of a load point shift strategy. The different performances of architectures C1 and C2 are due to the engine frictions, which in C1 diminish the regenerative braking efficiency and require more power in electric driving phases.

The results of the “NO<sub>x</sub> cut” strategy are shown in Fig. 17, where further improvements in NO<sub>x</sub> emissions in comparison with the conventional strategy can be clearly seen. On the other hand, fuel consumption penalties to be paid may range from affordable (2% for architecture E) to unacceptable (11% for architecture D). Architecture C2, which provided the highest fuel consumption and NO<sub>x</sub> emissions reductions with the conventional power management strategy, remains the best option also with the NO<sub>x</sub> cut strategy, although its results are now approached also by architecture E, the fuel consumption of which increases by only 3% while NO<sub>x</sub> emissions fall down of about 6%. Only architecture C1 (and architecture B, obviously, which does not have other capabilities beyond the start&stop) does not seem to get any emission advantage from the NO<sub>x</sub> cut strategy; again, the main reason could be the poor efficiency of the regenerative braking, due to the unavoidable ICE motoring, which is subtracting a remarkable amount of energy. For this reason, the ICE is therefore called, through load point shift, to store in the battery a huge amount of energy that will be then consumed in the EUDC segment in order to assist the ICE with the MGU. On the contrary, for all the other architectures the regenerative braking is very efficient and the ICE has therefore to generate a smaller energy quantity.

Finally, the analysis through numerical simulations of the potentialities of different hybrid powertrains highlighted that diesel hybrid powertrains, although being subject to NO<sub>x</sub> emissions constraints that could jeopardize their benefits, offered substantial advantages both in NO<sub>x</sub> emissions and in fuel consumption reduction. FAS (Flywheel Starter Alternator) with double clutch and the hybrid architecture with a MGU directly connected to the differential case by a dedicated gear were able to achieve the lowest fuel consumption levels.

## 5. Conclusions

In conclusion, ground transportation industry has nowadays accepted the reality that fast, efficient, and cost effective engine and vehicle development necessitates the use of numerical simulation at every stage of the design. Within the vehicle powertrain design and development process, different modelling approaches can be followed, depending on the simulation targets, ranging from fully dynamic, high fidelity models to black-box faster than real time models: it is therefore of crucial importance a clear target setting for the simulation activity, so to allow the selection of the most suitable modelling approach, in order to achieve the best compromise between detail level and computational requirements. The two case studies presented in the last section clearly support these statements: the first analysis, focusing on the evaluation of vehicle performance, requires a detailed description of the powertrain dynamics, such as turbo-lag phenomena, while the second, aiming to the assessment of the fuel economy potential of different Hybrid Electric Vehicle architectures

can exploit a simpler quasi-static approach since the analysis deals only with driving cycles with moderate dynamics.

Despite of these significant differences both models can provide valuable information to effectively support the powertrain development.

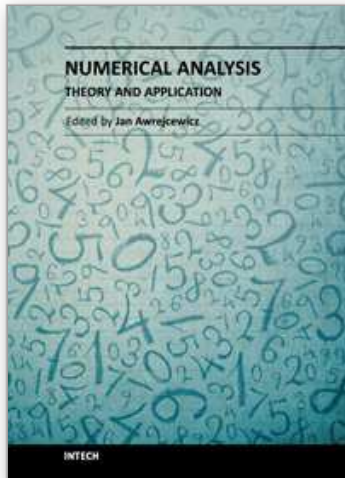
## 6. Nomenclature

AC	Alternative Current
BSFC	Brake Specific Fuel Consumption
BMEP	Brake Mean Effective Pressure
CFD	Computational Fluid Dynamics
DCT	Dual Clutch Transmission
EC	European Commission
ECU	Electronic Control Unit
EGR	Exhaust Gas Recirculation
EM	Electric Machine
EUDC	Extra Urban Driving Cycle
EV	Electric Vehicle
FAS	Flywheel Alternator Starter
FTP	Federal Test Procedure
GB	Gearbox
HEV	Hybrid Electric Vehicle
HIL	Hardware in the Loop
ICE	Internal Combustion Engine
MGU	Motor Generator Unit
MT	Manual Transmission
PID	Proportional Derivative Integrative (controller)
NEDC	New European Driving Cycle
NOx	Nitrogen Oxides
SIL	Software in the Loop
SOC	State of Charge
VGT	Variable Geometry Turbine

## 7. References

- Andrzejewski, R. Awrejcewicz, J. (2005), *Nonlinear Dynamics of a Wheeled Vehicle*. Springer-Verlag, Berlin.
- BOSCH R., (2011), *Bosch Automotive Handbook*, (8<sup>th</sup> Edition), Bentley Publishers, ISBN: 978-0-7680-4851-3.
- Canova, M., Gambarotta, A., (2002) *Automotive engine modelling for real -time control using an object-oriented simulation library*, 2<sup>nd</sup> Int. Workshop on Modelling, Emissions and Control of Automotive Engines-MECA02, Salerno, Italy.
- Chiodi, M., (2010) *An innovative 3D-CFD-Approach towards Virtual development of Internal Combustion Engines*, PhD Dissertation University of Stuttgart, Germany.
- Coltro, R., (2005) *Experimental investigation on the impact of engine characteristics on the vehicle behaviour during tip-in manoeuvres*, Mechanical Engineering Graduation Thesis, Politecnico di Torino, Turin, Italy, (in Italian).

- Cooper, B., Bar, F., Beasley, M., and Penny, I., (2009) *The Challenge of CO2 and Emissions Targets for Diesel Engines: Can Both Be Combined?* 9<sup>th</sup> Stuttgart International Symposium on Automotive and Engine Technology, Stuttgart, Germany.
- Gambarotta, A., (2001) *A Control-Oriented Library for the Simulation of Automotive Diesel Engines*, 3<sup>rd</sup> Int. Conference on Control and Diagnostics in Automotive Applications, Sestri Levante, Italy.
- GAMMA TECHNOLOGY, (2009) *GT-Suite User Manuals*, Chicago, United States.
- Genta, G. (1997) *Motor Vehicle Dynamics: Modeling and Simulation*, World Scientific Pub Co Inc, ISBN: 9789810229115, Singapore.
- González-Longatt, F. M. (2006) *Circuit Based Battery Models: A Review*, Proceedings of 2<sup>nd</sup> Congreso Iberoamericano De Estudiantes de Ingenieria Electrica, Puerto la Cruz, Venezuela.
- Guzzella, G., Sciarretta, A., (2007) *Vehicle Propulsion Systems: Introduction to Modeling and Optimization*, Springer, ISBN: 9783642094156, Berlin.
- Keribar, R., Ciesla C., and Morel, T., (2000) *Engine/Powertrain/Vehicle Modeling Tool Applicable to all Stages of the Design Process*, SAE Technical Paper 2000-01-0934.
- Millo, F., Badami, M., Ferraro, C.V., Rolando, L., (2009) *Different Hybrid Powertrain Solutions for European Diesel passenger cars*, SAE INTERNATIONAL JOURNAL OF ENGINES, 2009, Vol. 2, pages 493 - 504, ISSN: 1946-3936.
- Millo, F., M Badami, M., Ferraro, C.V., Lavarino, G., Rolando, L., (2010) *A Comparison Between Different Hybrid Powertrain Solutions for an European Mid-Size Passenger Car*, SAE Technical Paper 2010-01-0818.
- Morel, T., Keribar, R. and Leonard, A., (2003) *Virtual Engine/Powertrain/Vehicle Simulation Tool Solves Complex Interacting System Issues*, SAE Technical Paper 2003-01-0372.
- Pettiti, M., Pilo, L., Millo, F., (2007) *Development of a new mean value model for the analysis of turbolag phenomena in automotive diesel engines*, SAE Technical Paper 2007-01-1301.
- Serrao, L., (2009) *A Comparative Analysis of Energy Management Strategies for Hybrid Electric Vehicle*, PhD thesis, The Ohio State University, Columbus, Ohio, United States.
- Szumanowski, A., (2000), *Fundamentals of Hybrid Vehicle Drives*, Radom, ISBN: 372041148, Warsaw, Poland.
- Vassallo, A., Cipolla, G., Mallamo, F., Paladini, V., Millo, F., Mafrici, G., (2007) *Transient Correction of Diesel Engine Steady-State Emissions and Fuel Consumption Maps for Vehicle Performance Simulation*, 16<sup>th</sup> Aachener Kolloquium Fahrzeug und Motorentechnik, Aachen, Germany.



## **Numerical Analysis - Theory and Application**

Edited by Prof. Jan Awrejcewicz

ISBN 978-953-307-389-7

Hard cover, 626 pages

**Publisher** InTech

**Published online** 09, September, 2011

**Published in print edition** September, 2011

Numerical Analysis – Theory and Application is an edited book divided into two parts: Part I devoted to Theory, and Part II dealing with Application. The presented book is focused on introducing theoretical approaches of numerical analysis as well as applications of various numerical methods to either study or solving numerous theoretical and engineering problems. Since a large number of pure theoretical research is proposed as well as a large amount of applications oriented numerical simulation results are given, the book can be useful for both theoretical and applied research aimed on numerical simulations. In addition, in many cases the presented approaches can be applied directly either by theoreticians or engineers.

### **How to reference**

In order to correctly reference this scholarly work, feel free to copy and paste the following:

Federico Millo, Luciano Rolando and Maurizio Andreatta (2011). Numerical Simulation for Vehicle Powertrain Development, Numerical Analysis - Theory and Application, Prof. Jan Awrejcewicz (Ed.), ISBN: 978-953-307-389-7, InTech, Available from: <http://www.intechopen.com/books/numerical-analysis-theory-and-application/numerical-simulation-for-vehicle-powertrain-development>

**INTECH**  
open science | open minds

### **InTech Europe**

University Campus STeP Ri  
Slavka Krautzeka 83/A  
51000 Rijeka, Croatia  
Phone: +385 (51) 770 447  
Fax: +385 (51) 686 166  
[www.intechopen.com](http://www.intechopen.com)

### **InTech China**

Unit 405, Office Block, Hotel Equatorial Shanghai  
No.65, Yan An Road (West), Shanghai, 200040, China  
中国上海市延安西路65号上海国际贵都大饭店办公楼405单元  
Phone: +86-21-62489820  
Fax: +86-21-62489821

© 2011 The Author(s). Licensee IntechOpen. This chapter is distributed under the terms of the [Creative Commons Attribution-NonCommercial-ShareAlike-3.0 License](#), which permits use, distribution and reproduction for non-commercial purposes, provided the original is properly cited and derivative works building on this content are distributed under the same license.

IntechOpen

IntechOpen